OPTICAL PROPERTIES OF Ag DOPED Bi_2WO_6 NANOPLATES SYNTHESIZED BY HYDROTHERMAL PROCESS

A. PHURUANGRAT[a*], P. DUMRON GROJTHANATH[b], B. KUNTALUE[c],
T. THONGTEM[b,d] S. THONGTEM[d,e]

[a]*Department of Materials Science and Technology, Faculty of Science,
Prince of Songkla University, Hat Yai, Songkhla 90112, Thailand*
[b]*Department of Chemistry, Faculty of Science, Chiang Mai University,
Chiang Mai 50200, Thailand*
[c]*Electron Microscopy Research and Service Center, Faculty of Science,
Chiang Mai University, Chiang Mai 50200, Thailand*
[d]*Materials Science Research Center, Faculty of Science, Chiang Mai University,
Chiang Mai 50200, Thailand*
[e]*Department of Physics and Materials Science, Faculty of Science,
Chiang Mai University, Chiang Mai 50200, Thailand*

In this research, 0, 1 and 3 mol % Ag doped Bi_2WO_6 crystalline products were synthesized by hydrothermal process. The effects of Ag dopant on the structural and optical properties were studied by an X-ray diffractometer (XRD), a transmission electron microscope (TEM), an X-ray photoelectron spectroscopy (XPS) analyzer and a UV-visible spectrometer. The XRD patterns were specified as crystalline structure of Russellite Bi_2WO_6. TEM images revealed the presence of the products in the shape of nanoplates. The Bi_2WO_6 and 3 mol % Ag doped Bi_2WO_6 show strong absorption in the visible light region with the energy gaps of 3.34 and 3.42 eV, respectively.

1. Introduction

The Aurivillius family of layered bismuth oxide is generally formulated as $(Bi_2O_2)^{2+}(A_{m-1}B_mO_{3m+1})^{2-}$, where A is a mono-, bi- or tri-valent ion, B denotes a tetra-, penta- or hexa-valent ion, and m is the number (1, 2, 3, …..) of BO_6 octahedrons in each pseudo-perovskite block [1, 2]. For the simplest member of the Aurivillius family, m equals 1 with the structure consisting of perovskite $(WO_4)^{2-}$ layers lying in between $(Bi_2O_2)^{2+}$ layers [3, 4]. Bi_2WO_6 is very interesting semiconducting material because it has excellent physical and chemical properties: ferroelectricity [3, 5, 6], piezoelectricity [5, 6], pyroelectricity [6], nonlinear dielectric susceptibility [6, 7], photocatalytic activity [2, 8], luminescence and phonon properties [9, 10]. In this research, undoped and sliver doped Bi_2WO_6 have been synthesized by hydrothermal method. The effect of Ag doping on the structural and optical properties have been investigated.

2. Experimental Procedure

All chemicals were of analytical grade and were used without further purification. In a typical synthesis, 5 mmol sodium tungstate $(Na_2WO_4 \cdot 2H_2O)$ and 5 mmol bismuth nitrate $(Bi(NO_3)_3 \cdot 5H_2O)$ were separately dissolved in 50 ml deionized water to form two solutions, which

---

*Corresponding authors: phuruangrat@hotmail.com

will be slowly mixed together. Subsequently, 20 ml of 3 mol % silver nitrate ($AgNO_3$) was added to the aqueous solution mixture which was stirred for 20 min. Then the mixed solution pH was adjusted to 10 using 3 M NaOH. The following of 30 min stirring is the transfer of reaction solution into a 200 ml Teflon-lined autoclave. Similarly, the aqueous solution mixtures with 1 mol % Ag and without silver nitrate adding were done as well. The autoclaves were put in an oven and heated at 180 °C for 20 h. In the end, the system was naturally cooled to room temperature. The precipitates were collected, washed with distilled water and absolute ethanol several times, and dried in a drying cabinet at 80 °C for 5 h for further characterization.

X-ray powder diffraction (XRD) patterns of the products were recorded on a Philips PANanalytical X'Pert 2000 X-ray diffractometer with graphite monochromator and Cu K_α radiation ($\lambda = 0.154056$ nm) at a scanning rate of 0.02 deg/s ranging from 10 to 80 deg. The morphologies of the products were observed by a JEOL JEM-2010 transmission electron microscope (TEM) operating at 200 kV. Energy dispersive X-ray (EDX) spectrum and selected area electron diffraction pattern (SAED) were recorded along with the particle image analysis. X-ray photoelectron spectroscopic (XPS) measurement was carried out by a spectrometer (S/N:10001, Prevac Poland) with a VG Scienta R3000 hemispherical electron energy analyzer. The spectra were taken using Al K_α (1486.6 eV) radiation as an X-ray source. Absorption spectra in UV-visible region were taken by a Perkin Elmer Lambda 25 UV-visible spectrophotometer.

3. Results and Discussion

XRD patterns of Bi_2WO_6 and 3 mol % Ag doped Bi_2WO_6 products synthesized by the hydrothermal method are shown in Fig. 1. The dominant peaks at 2θ of about 28.3°, 32.7°, 47.1°, 55.8°, 58.5°, 68.7°, 75.9° and 78.3° were detected which were specified as crystalline structure of Russellite Bi_2WO_6 (JCPDS database no.: 79-2381), corresponding to the Miller indices of the (131), (002), (202), (133), (262), (004), (333) and (460) planes of bismuth tungstate, respectively [11]. The sharp strong diffraction peaks reveal that the as-synthesized products are well crystallized. No other characteristic diffraction peaks of impurities, such as Bi_2O_3 or WO_3, were detected, implying that the pure phase of Bi_2WO_6 could be synthesized by the simple hydrothermal method. The average size of un-doped Bi_2WO_6 and 3 mol % Ag doped Bi_2WO_6 products was calculated using the Scherrer formula: $D = K\lambda / \beta cos\theta$ [12, 13], where K = Scherer coefficient (0.89), β = the full width at half maximum (FWHM) of the main peak, λ = the wavelength of X-ray (1.5406 Å) and θ = the Bragg diffraction angle of the (131) main peak, with the particle size of 311 nm for Bi_2WO_6 and 300 nm for 3 mol % Ag doped Bi_2WO_6. It should be noted that no silver peak was detected in the doped product. Possibly, Ag content is too low to be detected by the XRD analysis.
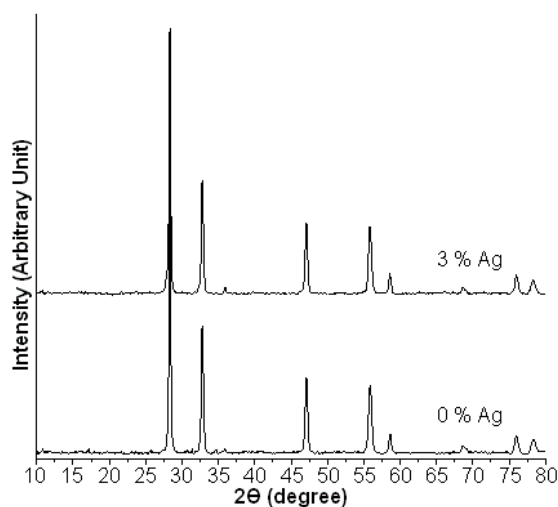

Fig. 1. XRD patterns of Bi_2WO_6 and 3 mol % Ag doped Bi_2WO_6.

To confirm the existence of silver in the 3 mol % Ag doped Bi_2WO_6 product, XPS was performed for the analysis (Fig. 2). The as-synthesized Ag doped Bi_2WO_6 powder shows 4f binding energies for Bi at 159.05 and 164.39 eV which were attributed to Bi $4f_{7/2}$ and Bi $4f_{5/2}$ [14, 15] of Bi^{3+} ions in the crystalline structure, respectively. The W 4f core level spectrum recorded on the crystal shows two components associated with $4f_{5/2}$ and $4f_{7/2}$ spin-orbit doublet at 37.5 and 35.4 eV, respectively. They could be specified as the +6 oxidation state of tungsten, in accordance with the previous reports [16, 17]. The O 1s region of 3 mol % Ag doped Bi_2WO_6 was fitted to three peaks, attributed to oxygen species in the lattice oxygen (529.92 eV), –OH hydroxyl groups (530.88 eV) and chemisorbed water (531.81 eV) [14, 16, 18]. The binding energies of Ag $3d_{5/2}$ and Ag $3d_{3/2}$ of the Ag doped Bi_2WO_6 product were detected at 368.50 and 374.40 eV which were clearly shifted to the higher binding energy, comparing to the Ag^0 binding energies of Ag $3d_{5/2}$ and Ag $3d_{3/2}$ for bulk Ag at about 367.2 and 374.2 eV, respectively [19]. The peak intensity of metallic silver is very low as compared to that of bismuth. The result is attributed to the low silver content in the crystal. The presence of Ag 3d peaks implies that silver was successfully doped into the Bi_2WO_6 matrix. They should be noted that binding energy of Ag $3d_{5/2}$ of Ag−Zn−O (369.2 eV) is higher than that of Ag^0 $3d_{5/2}$ (368.2 eV) [20, 21].
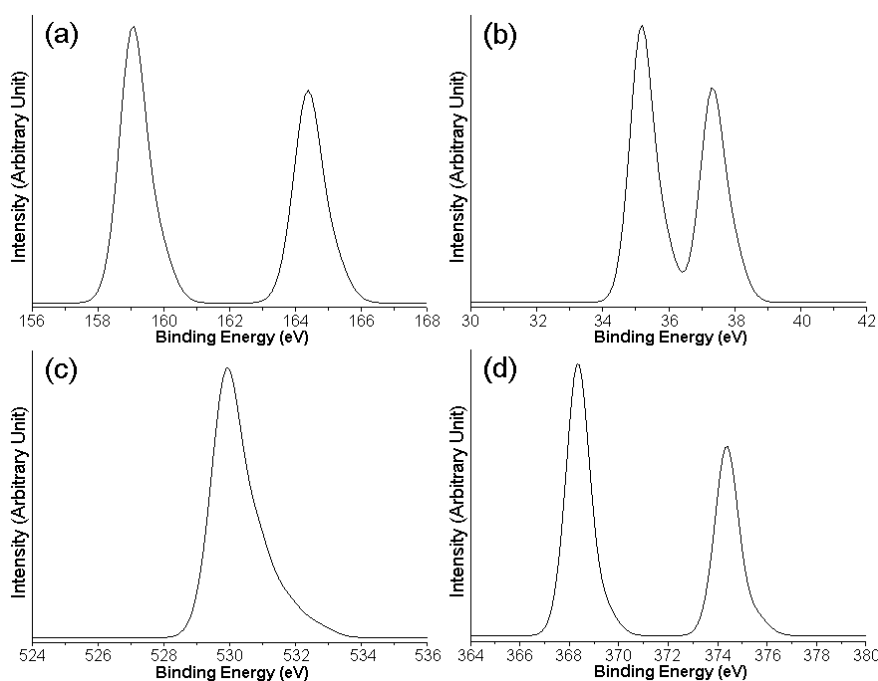

Fig. 2. XPS spectra of (a) Bi 4f, (b) W 4f, (c) O 1s, and (d) Ag 3d of 3 mol % Ag doped Bi_2WO_6.

The morphology of Bi_2WO_6 products containing different silver contents was characterized by TEM as shown in Fig. 3. For pure Bi_2WO_6 product, it was composed of a number of rectangular shaped nanoplates with an average edge length of 200−400 nm and thickness of 20 nm. No significant difference was observed between the pure Bi_2WO_6 and Ag-Bi_2WO_6 composites containing various Ag contents. In this research, Ag dopant did not change the morphology of Bi_2WO_6. The SAED pattern of 3 mol % Ag doped Bi_2WO_6 shows systematic spots of electron diffraction. This pattern clearly demonstrates single crystalline nature of the rectangular nanoplate. The crystalline zone axis was in the [001] direction, calculated from the SAED pattern of the 2D nanoplate. According to the present analysis, the nanoplate preferentially grew across the (001) plane, in parallel to its a x b layer. The two planar surfaces correspond to the (001) planes with one on the top and the other at the bottom. Possibly, four edges of the Bi_2WO_6 nanoplate were surrounded with the (110), (−110), (1−10) and (−1−10) planes. Energy

dispersive X-ray (EDX) analysis was employed in determining the composition of the 3 mol % Ag doped Bi_2WO_6 product. Its spectrum shows peaks of Bi (2.42 keV (M_α) and 2.53 keV (M_β)); W (1.78 keV (M_α), 1.84 keV (M_β), 8.40 keV (L_α), 9.67 keV ($L_{\beta1}$) and 9.96 keV ($L_{\beta2}$)); Ag (2.98 keV (L_α), 3.15 keV ($L_{\beta1}$) and 3.35 keV ($L_{\beta2}$)); and O (0.53 keV ($K_{\alpha1,2}$ and K_{ab})), confirmed the correspondence with the obtained Ag-Bi_2WO_6 composites.
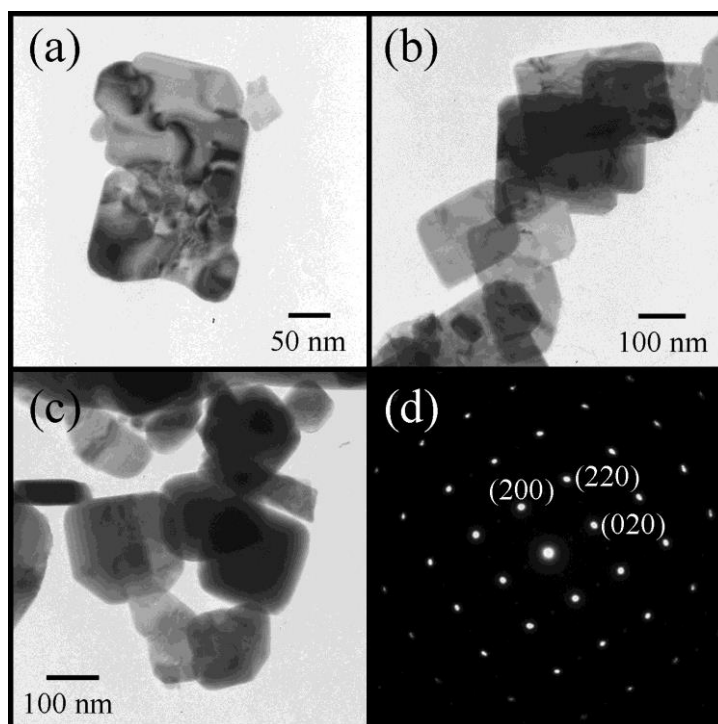

Fig. 3. TEM images of (a) Bi_2WO_6, (b) 1 mol % Ag doped Bi_2WO_6 and (c) 3 mol % Ag doped Bi_2WO_6; and (d) SAED pattern of 3 mol % Ag doped Bi_2WO_6.
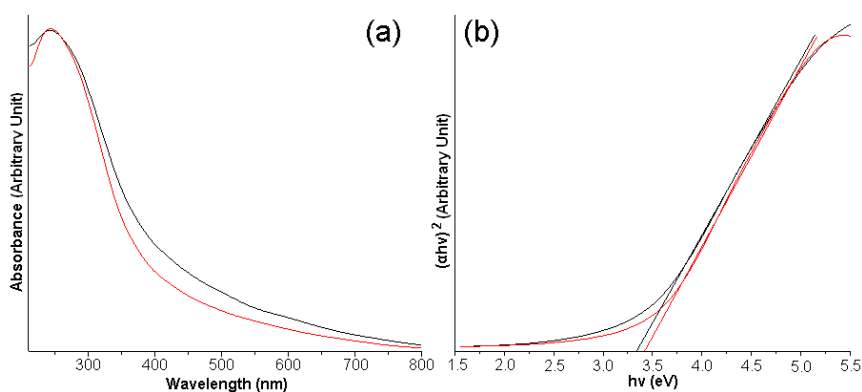

Fig. 4. (a) UV-visible absorption and (b) the plot of $(\alpha h\nu)^2$ against photon energy (hv) of Bi_2WO_6 (black) and 3 mol % Ag doped Bi_2WO_6 (red).

The optical absorption of Bi_2WO_6 and 3 mol % Ag doped Bi_2WO_6 was determined by a UV-visible spectrometer, as shown in Fig. 4(a). The as-synthesized Bi_2WO_6 and 3 mol % Ag doped Bi_2WO_6 show strong absorbance in the visible photonic region. UV-visible spectra of Bi_2WO_6 and 3 mol % Ag doped Bi_2WO_6 were similar absorbance ranging from ~200 to 800 nm. As a crystalline semiconductor, optical absorption near band edge follows the equation $\alpha h\nu = A(h\nu - E_g)^{n/2}$. The parameter n is determined by the transition characteristics in the semiconductor [22, 23]. When n equals 1, the absorption is direct transition. The band gaps can be estimated from

the plot of $(\alpha h v)^2$ vs photonic energy (hv) as shown in Figure 4(b), and were calculated to be about 3.34 eV for Bi_2WO_6 and 3.42 eV for 3 mol % Ag doped Bi_2WO_6.

4. Conclusions

In conclusion, 0, 1 and 3 mol % Ag doped Bi_2WO_6 nanoplates were successfully synthesized via a simple hydrothermal process. XRD patterns and TEM images of Bi_2WO_6 and 3 mol % Ag doped Bi_2WO_6 indicated the good crystalline Russellite structure. The XPS results revealed that silver was successfully doped into the crystalline matrix. The Bi_2WO_6 and 3 mol % Ag doped Bi_2WO_6 show strong absorption in the visible light region with their calculated energy gaps of about 3.34 eV for Bi_2WO_6 and 3.42 eV for 3 mol % Ag doped Bi_2WO_6.

Acknowledgement

References

[1] X.J. Wang, Z.Q. Gong, J. Zhu, X.B. Chen, Chinese. Phys. B **18**, 803 (2009).
[2] A. Phuruangrat, P. Dumrongrojthanath, N. Ekthammathat, S. Thongtem, T. Thongtem, J. Nanomater. **2014**, 1 (2014) Article ID 138561.
[3] X. Wang, L. Chang, J. Wang, N. Song, H. Liu, X. Wan, Micro. Nano. Lett. **7**, 1129 (2012).
[4] S.M.M. Zawawi, R. Yahya, A. Hassan, H.N.M.E. Mahmud, M.N. Daud, Chem. Cent. J. **7**, 1 (2013).
[5] T. Zeng, H. Yan, H. Ning, J. Zeng, M.J. Reece, J. Am. Ceram. Soc. **92**, 3108 (2009).
[6] B. Muktha, T.N.G. Row, J. Chem. Sci. **118**, 43 (2006).
[7] H. Djani, P. Hermet, P. Ghosez, J. Phys. Chem. C **118**, 13514 (2014).
[8] P. Dumrongrojthanath, T. Thongtem, A. Phuruangrat, S. Thongtem, Superlattice. Microstr. **54**, 71 (2013).
[9] M. Maczka, A.F. Fuentes, K. Hermanowicz, L. Macalik, P.E. Tomaszewski, L. Kepińiski, R. Lisiecki, J. Nanosci. Nanotechno. **1**0, 5746 (2010).
[10] O.M. Bordun, A.T. Stetshiv, T.M. Yaremchuk, Ukrainian J. Phys. **49**, 991 (2004).
[11] Powder Diffract. File, JCPDS Internat. Centre Diffract. Data, PA 19073–3273, U.S.A. (2001).
[12] A. Phuruangrat, S. Thongtem, T. Thongtem, B. Kuntalue, Dig. J. Nanomater. Bios. **7**, 1413 (2012).
[13] A. Phuruangrat, T. Thongtem, S. Thongtem, Mater. Sci. Poland **28**, 557 (2010).
[14] A. Phuruangrat, N. Ekthammathat, B. Kuntalue, P. Dumrongrojthanath, S. Thongtem, T. Thongtem, J. Nanomater. **2014**, 1 (2014) Article ID 934165.
[15] W. Wu, S. Liang, L. Shen, Z. Ding, H. Zheng, W. Su, L. Wu, J. Alloy. Compd. **52**0, 213 (2012).
[16] Y. Zhang, W. He, H. Zhao, P. Li, Vacuum **95**, 30 (2013).
[17] C. Li, G. Chen, J. Sun, Y. Feng, J. Liu, H. Dong, Appl. Catal. B **163**, 415 (2015).
[18] L. Liu, Y. Wang, W. An, J. Hu, W. Cui, Y. Liang, J. Mol. Catal. A **394**, 309 (2014).
[19] Y. Cai, H. Fan, M. Xu, Q. Li, Colloid. Surf. A **436**, 787 (2013).

[20] O. Lupan, L. Chow, L.K. Ono, B.R. Cuenya, G. Chai, H. Khallaf, S. Park, A. Schulte, J. Phys. Chem. C **1144**, 12401 (2010).
[21] J. Lu, H. Wang, S. Dong, F. Wang, Y. Dong, J. Alloy. Compd. **617**, 869 (2014).
[22] T. Thongtem, S. Kungwankunakorn, B. Kuntalue, A. Phuruangrat, S. Thongtem, J. Alloy. Compd. **506**, 475 (2010).
[23] O. Yayapao, T. Thongtem, A. Phuruangrat, S. Thongtem, J. Alloy. Compd. **509**, 2294 (2011).